Spectrochimica Acta Part A 78 (2011) 1476–1481

Contents lists available at ScienceDirect

Spectrochimica Acta Part A: Molecular and Biomolecular Spectroscopy

journal homepage: www.elsevier.com/locate/saa

Temperature dependent crystallographic transformations in chalcedony, SiO_2, assessed in mid infrared spectroscopy

Patrick Schmidt*, François Fröhlich

Muséum national d'histoire naturelle, Dpt. de Préhistoire UMR 7194, Centre de spectroscopie infrarouge, CP 57, 57, rue Cuvier, 75231 Paris Cedex 05, France

ARTICLE INFO

Article history:
Received 22 November 2010
Received in revised form 6 January 2011
Accepted 23 January 2011

Keywords:
Chalcedony
Flint
FT-IR
555 cm^{-1} band
Surface silanole
SiOH

ABSTRACT

Chalcedony consists of hydroxylated 50–100 nanometre measuring α-quartz (SiO_2) crystallites that lose their surface silanole groups (Si–OH) upon heating between 350 °C and 600 °C. The loss of the chalcedony's ≈1% of silanole groups allows for the healing of water related defects in the crystallites. We investigated these crystallographic transformations using Fourier Transform mid Infrared Spectroscopy in direct transmission, Attenuated Total Reflection (ATR) and the reflectivity. We found that an absorption band that is specific for chalcedony at 555 cm^{-1} disappears gradually upon heating between 350 °C and 600 °C. The reduction of the band is correlated to the loss of surface silanoles. This result leads to the assignment of the band to free Si–O vibrations in non bridging Si–OH groups that have a lower natural frequency than Si–O vibrations in bridging Si–O–Si. The recognition of a silanole signal in the mid infrared allows for an easy, cheap and rapid recognition of hydroxyl in chalcedony.

1. Introduction

Chalcedony consists of 50–100 nanometre measuring α-quartz crystallites [1] in a fibrous arrangement. When heated to temperatures above 600 °C, the chalcedony framework suffers structural transformations of two kinds. It loses all its water and the quartz lattice undergoes a phase transition. In quartz single crystals, this reversible phase transition between the α- and β-form takes place at 573 °C and 1 bar. After a first order transition, a typical single crystal passes through a 1.3 °C lasting incommensurate phase and accomplishes a second order transition to β-quartz at 574.3 °C [2,3]. These inversions cause sharp endothermic reactions in the Differential Thermal Analysis (DTA) of single crystals [4,5]. DTA of chalcedony shows somewhat less intense peaks that spread over a larger temperature interval [4]. This broadening can be explained by the high defect density and the strained nature of the crystallites that compose the chalcedony [1,6]. Clamping effects and surface relaxation result in parts of the chalcedony framework where the quartz lattice is subject to elevated pressure whereas other parts experience dilatation of the lattice. The pressure gradient can extend the inversion up to an interval of 100 °C [1]. The loss of almost all of the chalcedony's structural water occurs even before the high-low transition [7]. The total hydroxyl (OH) content of these rocks can be differentiated into molecular water (H_2O) and chemically bound silanoles (SiOH) [8,9]. These two types of 'water' account for up to 2% of the total mass of some chalcedonies [10]. Although H_2O is essentially evaporated at lower temperatures, some water molecules can be retained until above the phase transition [8]. Silanoles are progressively evaporated from 350 °C upward [9]. The majority is lost until approximately 600 °C [8]. The evacuation of hydroxyl (OH) from the quartz structure is expected to allow for the formation of new Si–O–Si bonds that were previously hindered by hydrogen protons [11]. The formation of new atomic bonds may lead to structural rearrangements in the quartz lattice.

A convenient way of investigating crystallographic transformations upon heating is infrared spectroscopy, for crystal vibrations are strongly influenced by temperature. In quartz single crystals, lattice bands in the mid-infrared become larger and loose detail upon heating. Some of the α-quartz bands disappear progressively when the α–β transition temperature is approached and are absent in the β-form [12]. When the sample is quenched to room temperature, the regular α-quartz spectrum is observed and no transformation in band shape is evident as compared with the spectra of unheated samples. Chalcedony, however, can be expected to show significant transformations in its spectrum after quenching from high temperature due to its structural differences with quartz single crystals. We investigated these transformations using Fourier Transform mid Infrared Spectroscopy (FTIR). The infrared spectra of chalcedony show the expected quartz absorptions, an additional band at 555 cm^{-1} and a change in morphology of the low frequency envelope [13] (Fig. 1). Transformations in band shape in the spectra of the quenched samples would correspond to a memory effect and indicate non reversible crystallographic transformations when the material is heated. The experiments

* Corresponding author. Tel.: +33 634281896.
E-mail address: schmidt@mnhn.fr (P. Schmidt).

1386-1425/$ – see front matter © 2011 Elsevier B.V. All rights reserved.
doi:10.1016/j.saa.2011.01.036

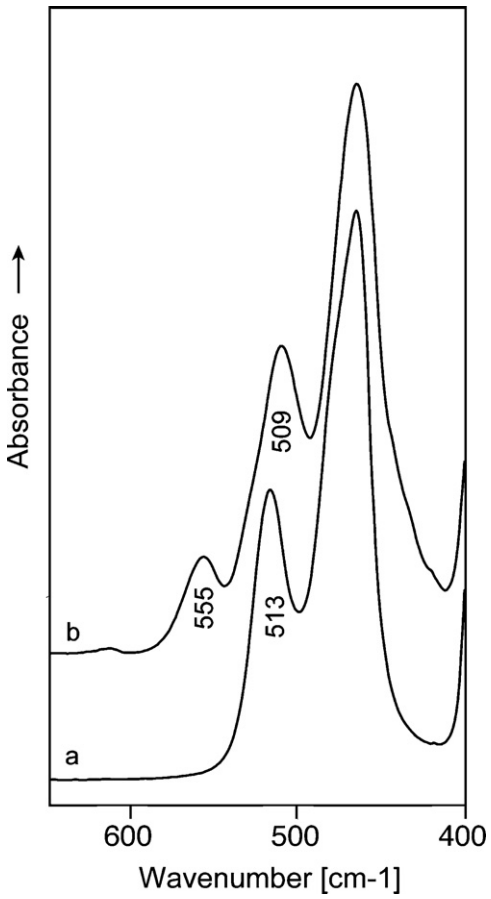

Fig. 1. Infrared transmission spectra showing the low frequency envelope in quartz and chalcedony, (a) quartz single crystal and (b) chalcedony sample R-GE-Cal. The figure resumes the main differences between α-quartz single crystals and chalcedony: the 555 cm^{-1} band and the wavenumber shift from 513 cm^{-1} to 509 cm^{-1}. Spectra vertically displaced.

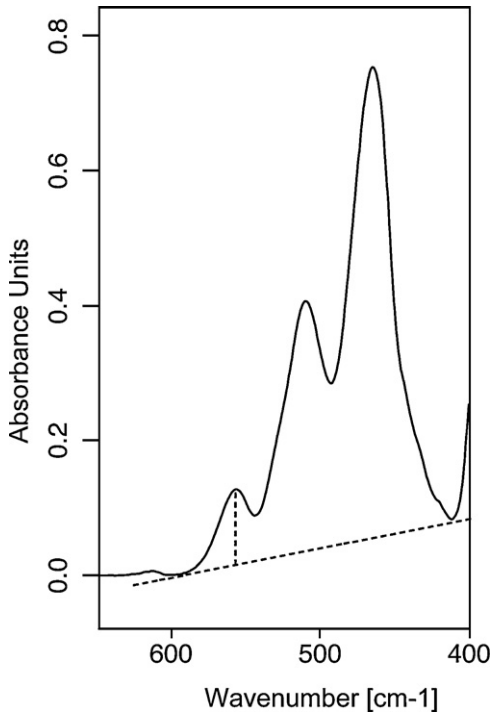

Fig. 2. Baseline for the absorbance of the 555 cm^{-1} band (dotted line) and the total integrated area under the low frequency envelope used for the transmission and ATR measurements. The baseline was a straight line between the two lowest points of the low frequency envelope.

subject to this work aim in assessing such transformations in chalcedony.

2. Materials and methods

2.1. Experimental and samples

Five samples of chalcedony and one sample of hydrous silica grass (opal-A, [14]) were analysed. The samples were broken into fragments weighing between 1 and 4 g. Each fragment was heated to a different temperature between 100 °C and 1000 °C in a Thermolyne 47900 electrical furnace with free access to oxygen. The exact protocols for each sample are resumed in Table 1. Analyses were started after the samples had cooled down to room temperature. Spectra were acquired with a Brucker VECTOR 22 FTIR spectrometer by means of direct transmission and Attenuated Total Reflection (ATR). Powders with a grain size <50 μm were used for the ATR measurements. The preparation for transmittance measurements (KBr pellets) was done with a grain size <2.5 μm, a concentration of 6×10^{-4} g in a pellet of 0.3 g (balance precision to 10^{-5} g) and controlled homogenisation of the sample powder and the KBr. Spectra were obtained between 1400 cm^{-1} and 400 cm^{-1} with a resolution of 2 cm^{-1}. The reflectivity in the mid infrared was measured with the same spectrometer. Spectra were acquired on diamond polished surfaces. The reflection coefficient (R) was measured at 45° with polarised radiation. The polarisation of the incident beam was such that the electric field was perpendicular to the plane of reflection. In order to evaluate the hydroxyl content of chalcedony at different temperatures, two additional samples were cut into thin slabs, diamond polished on both sides, and analysed in their Si–OH region in the near infrared (NIR) using direct transmission (for sample thicknesses see Table 1). Hydroxyl in chalcedony can be directly measured through a Si–OH combination band near 4500 cm^{-1} [10,15]. These measurements were carried out on the same spectrometer. Spectra were acquired between 4800 and 4200 cm^{-1} with a resolution of 8 cm^{-1}. The reflectivity at 555 cm^{-1} was measured on one of the sample's polished sides after the transmission measurement. Analyses were started after the samples had cooled down to room temperature. After this, the samples were heated to the next higher temperature before the transmission and reflection measurements recommenced.

2.2. Signal processing and error bars

The baseline for the measurement of the absorbance at 555 cm^{-1} band was a straight line drawn between the two lowest points on either side of the low frequency envelope (Fig. 2). In order to equate the obtained values, the intensity of the 555 cm^{-1} band was divided by the intensity of a strong band of the spectrum. The obtained indices are independent of potential errors, induced by water evacuation, changing porosity or any other weight loss on progressive heating. Error bars for the equated absorption index were determined by repeating the measurement several times for one sample. Ten pellets with different concentrations were pressed from the unheated sample R-GE-Cal. The maximal deviation from the arithmetic mean of the obtained values was used for error bars. This deviation was found to be appropriate for the transmittance and the ATR measurements. The deviations from the reflectance and NIR transmission values were determined by repeating the measurement ten times on a single sample. The baseline for the measure-

Table 1
Samples and annealing temperatures.

Technique	Sample	Description	Annealing temperatures (°C)
Transmission	R-GE-Cal	Botryoidal sedimentary length-fast chalcedony from a cavity in flint. From upper cretaceous chalk, *plage d'Étretat*, France	200, 300, 400, 450, 500, 525, 550, 600, 650, 700, 800, 900, 1000
Transmission	R-Cal-Pou	Hydrothermal length-fast chalcedony precipitated on quartz, *Puy de Dôme*, France	400, 450, 500, 550, 600, 650
Transmission	Cal-Biot	Hydrothermal geode filling of length-fast chalcedony, Biot, France	400, 450, 500, 550, 600, 650
Diamond ATR	R-Opal-A	Geyserite, Yellowstone Park, USA	Not heated
Diamond ATR	TR-S-01	Turonian fine flint, consisting of length-fast chalcedony. North of Tours, France	200, 250, 300, 350, 400, 450, 500, 550, 600
Reflectivity	PS-S-02	Turonian fine flint, consisting of length-fast chalcedony. East of Tours, France	200, 250, 300, 350, 400, 450, 500
NIR/reflectivity	PS-09-04	Coniacian black flint, Étretat, France Sample thickness: 545 ± 5 μm	100, 150, 200, 250, 300, 350, 400, 450, 500, 550, 600
NIR/reflectivity	PS-09-25	Brown upper Cretaceous Flint, *Le grand Pressigny*, France. Sample thickness: 998 ± 5 μm	100, 150, 200, 250, 300, 350, 400, 450, 500, 550, 600

ment of the absorbance at 4547 cm^{-1} was a straight line drawn between the two lowest points on either side of the absorption band.

3. Results

3.1. Transmittance and ATR

Spectra of the flint and chalcedony samples show the characteristic absorption bands of α-quartz single crystals in the low frequency region (Fig. 1). The chalcedony spectra show an additional absorption band at 555 cm^{-1} and a frequency shift of the Si–O–Si lattice band at 515 cm^{-1} (in α-quartz) to around 509 cm^{-1} as already reported by Badia and Fröhlich [13]. As shown in Fig. 3a and b, the 555 cm^{-1} band disappears upon heating and the wavenumber of the 515 cm^{-1} band shifts to values known for quartz single crystals. The majority of this evolution takes place between 350–400 °C and 600 °C. The results of the measurements on the annealed samples are plotted in Fig. 4a and b and show the progressive reduction of the 555 cm^{-1} band. A correlation between the disappearance of the band and the frequency shift of the quartz lattice band at 515–509 cm^{-1} is noticeable (Fig. 5). The

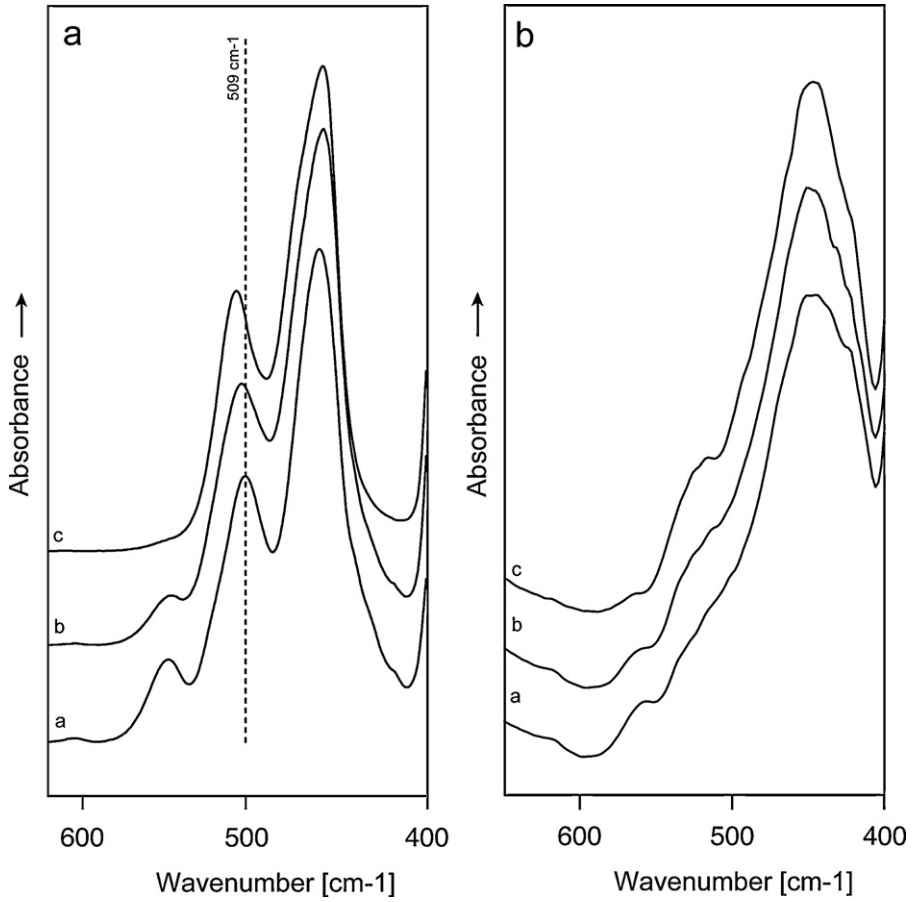

Fig. 3. Reduction of the 555 cm^{-1} band and frequency shift of the adjacent Si–O–Si band, (a) R-GE-Cal, transmission and (b) TR-S, ATR. Spectra are displaced vertically. Spectra (a) taken from unheated samples, spectra (b) of samples heated to 450 °C and spectra (c) of samples heated to 600 °C. Spectra (b) and (c) were acquired at room temperature after quenching the samples.

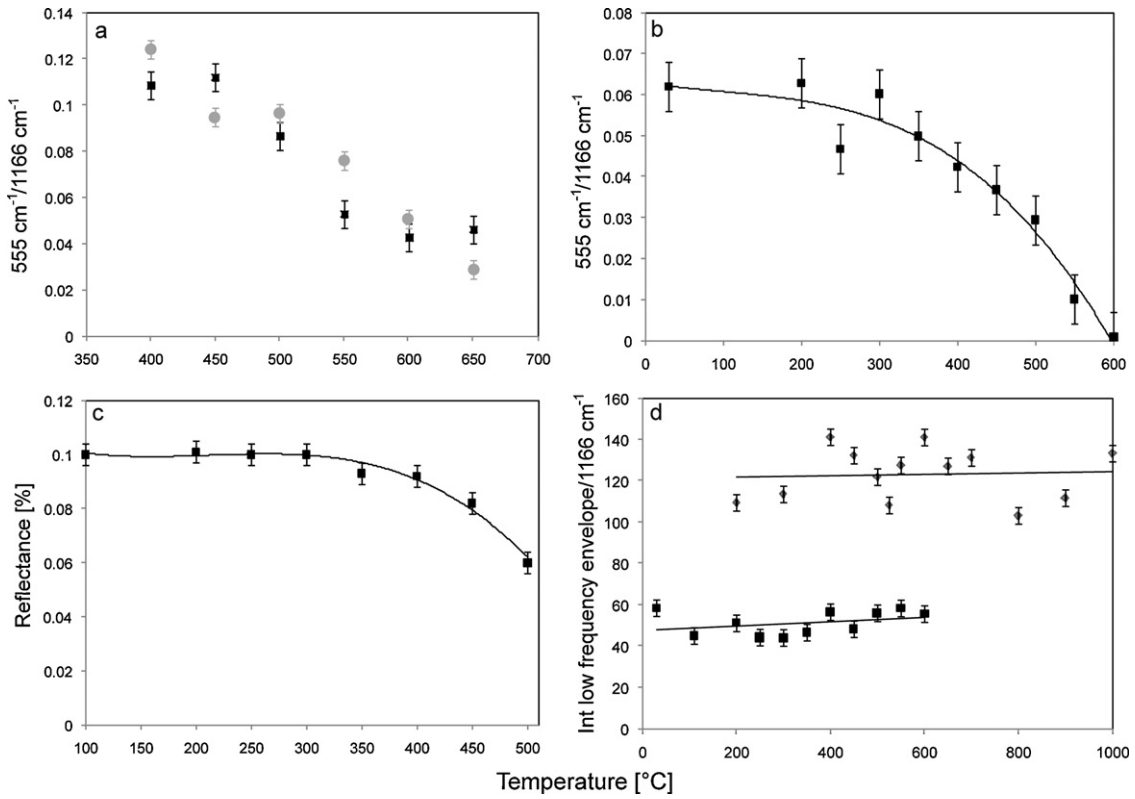

Fig. 4. Plots of the absorption index against temperature. (a) transmission measurements (round dots = Cal-Biot, square dots = R-Cal-Pou), (b) ATR of TR-S, (c) reflection on PS-S-02, and (d) the total integrated area under the low frequency envelope (grey dots = R-GE-Cal, black dots = TR-S). The absorption index is obtained by dividing the measured absorption by a strong lattice band that was found not to vary with temperature (see Section 2.1).

integrated total area under the low frequency envelope does not show any variation that can be correlated to the annealing temperature (Fig. 4d). The area remains unchanged when the 555 cm^{-1} band disappears. However, the obtained values of the integrated area show too high a dispersion for a precise statement and have to be considered as indications only. The spectrum of the opal-A sample also shows a band at 555 cm^{-1} (Fig. 6).

3.2. Reflectivity

The reflection coefficient (R) spectra also show the 555 cm^{-1} band that disappears with increasing temperature. The reduction

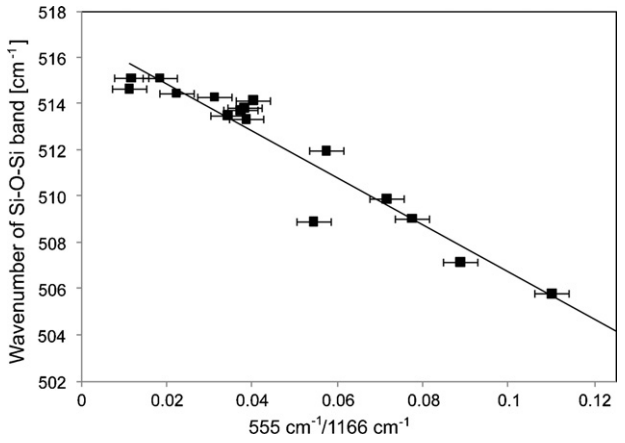

Fig. 5. Plot showing the correlation between the absorption index of the 555 cm^{-1} band and the frequency of the adjacent Si–O–Si band from the transmission spectra of sample R-GE-Cal.

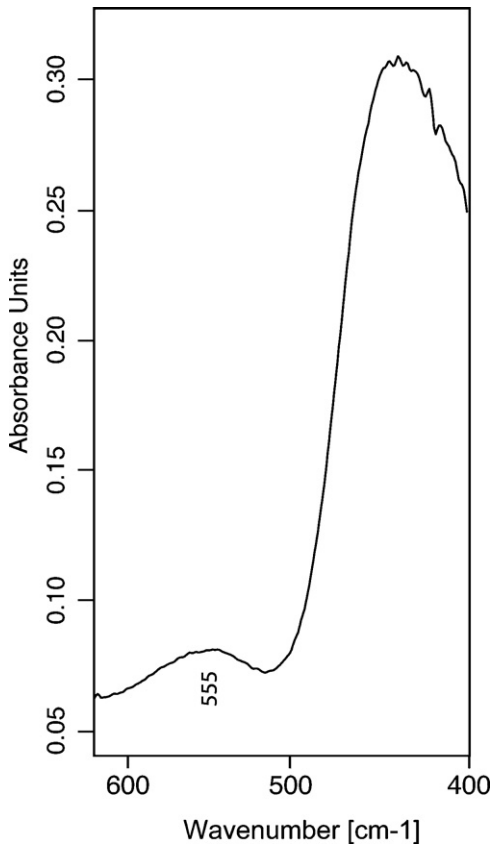

Fig. 6. ATR spectrum of sample R-Opal-A measured at room temperatures. The spectrum shows the 555 cm^{-1} band like chalcedony.

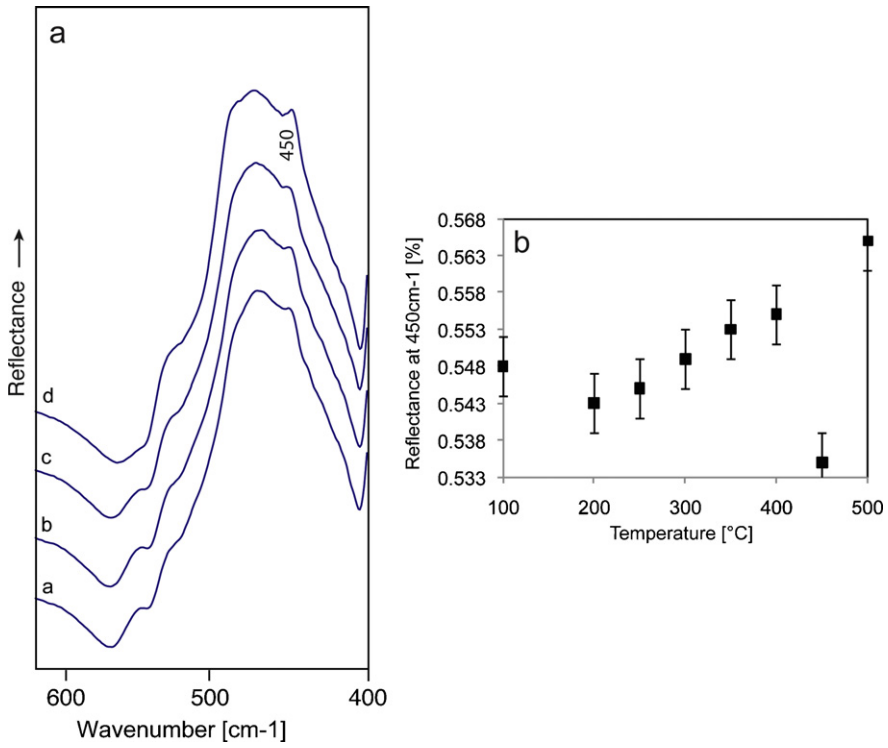

Fig. 7. (a) Spectra of the reflection coefficient of PS-S-02 showing the low frequency envelope, spectrum (a) taken from the unheated sample, (b) sample heated to 300 °C, (c) 400 °C and (d) 500 °C. Spectra (b), (c) and (d) were acquired at room temperature after quenching the samples. Spectra are displaced vertically. (b) Plot showing the increase in reflectivity at 450 cm^{-1} in function of the heating temperature.

of R at 555 cm^{-1} starts around 350 °C and is gradual until the highest measured temperature at 500 °C (Fig. 4c). Heating until higher temperatures was not possible, due to intense fracturing of the sample. The low frequency envelope shows evolution in its morphology at 530 cm^{-1} and 490 cm^{-1} (Fig. 7a). This morphology change might be the equivalent of the 515–509 cm^{-1} shift observed in the transmission measurements. The reflectivity at 450 cm^{-1} increases continuously between 473 K and 773 K (Fig. 7b).

3.3. SiOH NIR measurements compared with the reflectivity at 555 cm^{-1}

The SiOH combination band [15] in the near infrared undergoes a temperature dependent evolution. Fig. 8 shows the reduction of the band. The reflectivity at 555 cm^{-1} is reduced at the same time. The reduction of the two bands starts at 350 °C and the rhythm of its disappearance is very similar in both samples. Silanoles almost totally disappear at 600 °C. The 555 cm^{-1} band vanishes almost completely at this temperature. Fig. 9 shows the reduction of the 555 cm^{-1} band and the concomitant disappearance of the SiOH band at 4547 cm^{-1}.

4. Discussion

These results indicate non reversible crystallographic transformations in chalcedony upon heating. The starting and end temperature of the reduction of the 555 cm^{-1} band suggest that the α–β phase transition cannot account for the observed transformations alone. The transition is reported to be gradual in chalcedony [4,6] and Rios et al. [1] report the event to last from about 50 °C below to approximately 50 °C above 573 °C. The reduction of the

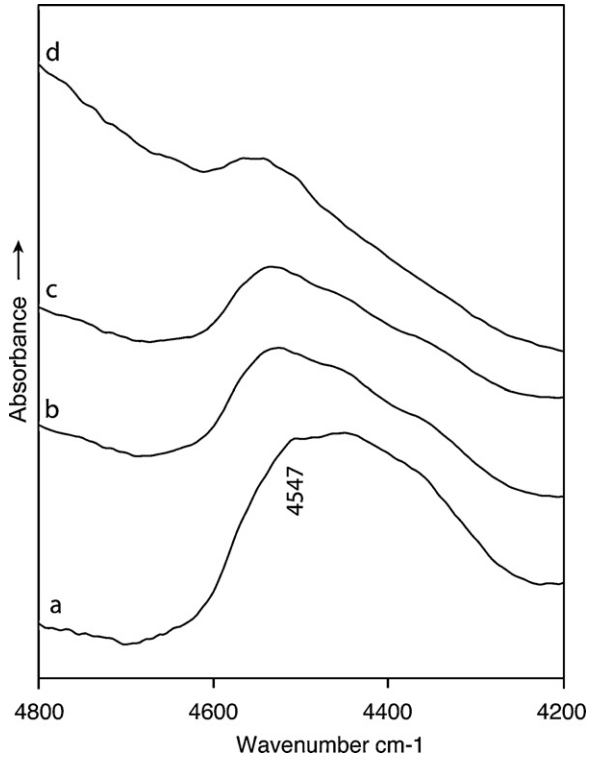

Fig. 8. Transmission spectra of the Si–OH combination band around 4500 cm^{-1}, (a) taken from the unheated sample PS-09-45 and (b) this sample heated to 400 °C, (c) 500 °C and (d) 600 °C. Sample thickness 998 ± 5 μm. Spectra (b), (c) and (d) were acquired at room temperature after quenching the sample. Spectra are displaced vertically.

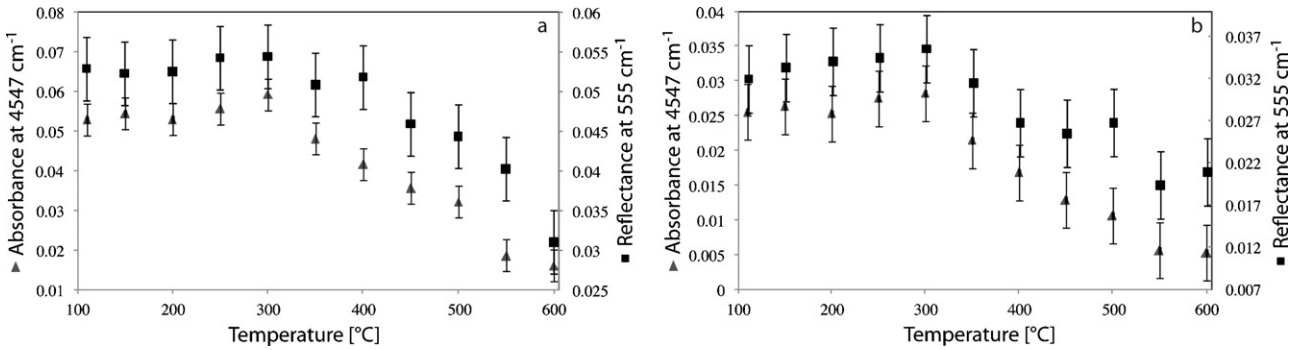

Fig. 9. Plots of the absorption at 4547 cm^{-1} (▲ triangles) and the reflectivity at 555 cm^{-1} (■ squares) against temperature. (a) PS-09-25, sample thickness 998 ± 5 μm; (b) PS-09-04, sample thickness 545 ± 5 μm. The measurements of the absorption and the reflectivity were acquired on the same samples. Scale to the left of the graphs: absorption at 4547 cm^{-1} (▲), scale to the left: reflectivity at 555 cm^{-1} (■). The starting temperature of the reduction of the two bands is 350 °C and the rhythm of their reduction shows their correlation.

555 cm^{-1} band, however, starts at much lower temperatures and is essentially finished at 600 °C. It seems therefore unlikely that the reduction of the band is due to structural rearrangement at the α/β transition.

A more likely interpretation of the observed transformations in chalcedony is the 'evaporation' of silanoles. The gradual disappearance of surface silanoles from 350 °C upwards [9] is concomitant with the reduction of the 555 cm^{-1} band. The majority of SiOH groups is lost around 600 °C [8–10]. This is also the temperature at which the band disappears almost totally. The direct NIR measurement of silanole at different temperatures shows a good correlation between the 555 cm^{-1} band and the SiOH content of the chalcedony samples. Thus, it seems that the 555 cm^{-1} absorption band is associated with the structural hydroxyl content of chalcedony. An additional argument for the assignment of the band to hydrogen defects is its occurrence in the opal-A sample. In addition to the Si–O and Si–O–Si absorption bands; this hydroxylated silica glass [16] shows a band at the same wavenumber as in chalcedony (ν = 555 cm^{-1}). The 555 cm^{-1} band may correspond to Si–O vibrations caused by non-bridging oxygen apices of SiO_4 tetrahedra. Non bridging Si–O bonds are formed when H^+ occupies the residual charge of non bridging $Si–O^-$, forming Si–OH. The resulting Si–O vibration is expected to have a higher natural frequency than Si–O vibrations in bridging Si–O–Si. This is because $\nu_{Si–O}$ in Si–OH is not directly influenced by another Si of the crystal lattice in its vicinity like it is the case for $\nu_{Si–O}$ in Si–O–Si. Bonding of Si–O with another Si of the lattice lowers $\nu_{Si–O}$ when compared to the free vibration in Si–OH. Such structural defects are expected to be numerous in chalcedony due to the high density of twin interfaces in the crystallites [17]. This kind of non-bridging Si–O bending vibration can also be expected in hydroxylated silica glass like opal-A where a part of the Si–O–Si bonds are interrupted by the incorporation of hydrogen protons [18]. The 555 cm^{-1} band in chalcedony is thus assigned to Si–O bending vibrations of non bridging Si–OH bonds whereas the Si–O vibrations of bridging Si–O–Si cause absorption at lower wavenumbers in the low frequency envelope. When the silanole groups disappear upon heating, new Si–O–Si bonds are formed [11]. The frequency of the vibration that formerly caused absorption at 555 cm^{-1} shifts back to the low frequency envelope. The observed correlation between the intensity of the 555 cm^{-1} band and the change of morphology of the low frequency envelope corroborate this.

5. Conclusion

Chalcedony undergoes non reversible crystallographic transformations when heated to temperatures higher than 350 °C. These transformations correspond to the 'evaporation', of surface silanoles (Si–OH). Such silanole groups cause a frequency shift of a part of the Si–O bond's vibrations to 555 cm^{-1}. The disappearance of Si–OH causes the reduction of the 555 cm^{-1} band and a transformation of the morphology of the low frequency envelope. This data allows interpreting the infrared spectrum of chalcedony as the one of hydroxylated α-quartz. The recognition of a silanole signal in the mid infrared allows for an easy, cheap and rapid recognition of hydroxyl in chalcedony. These results are of interest not only to thermodynamic research about chalcedony containing rocks but also to archaeometric research about the prehistoric heat treatment of silica rocks. Further experimentations on the high temperature behaviour of the 555 cm^{-1} band in hydroxylated silica glass will help the understanding of biogenic silica grass production.

References

[1] S. Rios, E.K.H. Salje, S.A.T. Redfern, The European Physical Journal B 20 (2001) 75–83.
[2] J.P. Bachheimer, Journal de Physique Lettres 41 (1980) 559–561.
[3] G. Dolino, J.P. Bachheimer, B. Berge, C.M.E. Zeyen, Journal de Physique 45 (1984) 361–371.
[4] O.F. Tuttle, American Mineralogist 34 (1949) 723–730.
[5] W. Smykatz-Kloss, W. Klinke, Journal of Thermal Analysis and Calorimetry 48 (1997) 19–38.
[6] C.R. Pelto, American Journal of Science 254 (1956) 32–50.
[7] H. Graetsch, in: P.J. Heaney, C.T. Prewitt, G.V. Gibbs (Eds.), Silica: Physical Behaviour, Geochemistry and Materials Applications. Reviews in Mineralogy, vol. 29, Mineralogical Society of America, Washington, 1994, pp. 209–232.
[8] C. Frondel, American Mineralogist 67 (1982) 1248–1257.
[9] H. Graetsch, O.W. Flörke, G. Miehe, Physics and Chemistry of Minerals 12 (1985) 300–306.
[10] O.W. Flörke, B. Köhler-Herbertz, K. Langer, I. Tönges, Contributions to Mineralogy and Petrology 80 (1982) 324–333.
[11] T. Moxon, S.J.B. Reed, Mineralogical Magazine 70 (2006) 485–498.
[12] F. Gervais, B. Piriou, Physical Review B 11 (1975) 3944.
[13] D. Badia, F. Fröhlich, Comptes rendus de l'Académie des Sciences 281 (1975) 85–88.
[14] J.B. Jones, E.R. Segnit, Journal of the Geological Society of Australia 18 (1971) 57–68.
[15] H. Scholze, Fortschritte der Mineralogie 38 (1960) 122–123.
[16] F. Fröhlich, Terra Nova 1 (1989) 267–273.
[17] G. Miehe, H. Graetsch, O.W. Flörke, Physics and Chemistry of Minerals 10 (1984) 197–199.
[18] K. Langer, O.W. Flörke, Fortschritte der Mineralogie 53 (1974) 17–51.